Compressive Sensing-Based Missing-Data-Tolerant Fault Detection for Remote Condition Monitoring of Wind Turbines

Yayu Peng, *Student Member, IEEE*, Wei Qiao, *Fellow, IEEE*,
and Liyan Qu, *Senior Member, IEEE*

***Abstract*—Compared with traditional onsite wind turbine condition monitoring systems, the remote condition monitoring systems can use better computational resources to process data with more advanced algorithms and, thus, can provide more advanced condition monitoring capabilities, but may suffer from a data loss problem, especially when wireless data transmission is used. To solve this problem, this paper proposes a compressive sensing-based missing-data-tolerant fault detection method for remote condition monitoring of wind turbines. First, the condition monitoring signals collected from wind turbines are conditioned to increase their sparsity. Then, a compressive-sensing-based sampling algorithm is designed to sample the conditioned signals. The resulting data samples, called measurements of the conditioned signals are transmitted wirelessly during which some data samples are possibly lost. At the data receiving end, the conditioned signals are reconstructed from the received data samples, which might be incomplete, via a compressive-sensing-based signal reconstruction algorithm. Finally, spectrum analysis is performed on the reconstructed signals for wind turbine fault detection via fault characteristic frequency identification. The proposed method is validated for bearing fault detection of a Skystream 3.7 wind turbine and an Air Breeze wind turbine by using the data of a generator current signal collected from each wind turbine remotely while considering different data loss rates.**

***Index Terms*—Compressive sensing, data loss, fault detection, fault tolerance, remote condition monitoring, wind turbine, wireless sensor network.**

I. INTRODUCTION

IT has been reported that premature component failure and unscheduled maintenance are key challenges facing the wind power industry [1]. In order to compete with conventional fossil fuel power plants, the reliability of wind turbines needs to be improved. It was pointed out in [2] that, with the help of a condition monitoring system (CMS), a fault in a wind turbine could be detected in the incipient stage so that preventive maintenance could be scheduled before a catastrophic failure occurs. This can significantly improve wind turbine availability and reliability, prolong wind turbine lifetime, and reduce the financial loss caused by unplanned shutdown.

Condition monitoring for wind turbines can be performed onsite, remotely, or both. The advantage of an onsite CMS is that by using the data processing and computing equipment installed onsite in the wind turbine being monitored, condition monitoring and fault diagnosis can be performed timely with little data communication cost or delay. However, due to the use of limited local data and limited computational resource, the condition monitoring capability of an onsite CMS is limited. On the contrary, the remote CMSs can use data collected from different wind turbines that contains more information of their health conditions and better computational resources to process the date using more advanced algorithms [3]-[5]. Thus, compared to the onsite CMSs, the remote CMSs are usually more capable and more reliable for wind turbine condition monitoring but require more expensive communication equipment for data transmission.

In a remote CMS, the condition monitoring data can be transmitted through a wired or wireless communication system. Compared to the wired communication systems, the wireless communication systems, such as those based on wireless sensor networks (WSNs), have the advantages of rapid deployment, easier installation, and lower costs [6]. These merits make WSNs promising for remote condition monitoring of highly distributed wind turbines, particularly offshore wind turbines. However, WSNs usually suffer a data loss problem due to radio interference, poor installation, poor antenna orientation, bad weather, or large transmission distance [7]. Fig. 1 illustrates the data loss problem of a signal collected for wind turbine condition monitoring in which the data samples in the two time windows are lost during wireless transmission. The locations of

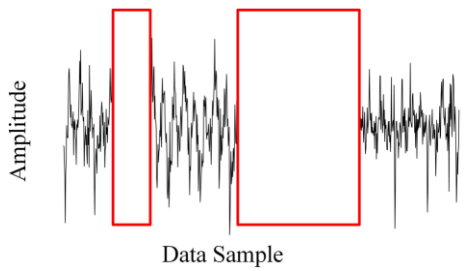

Fig. 1. Data loss problem in a wind turbine condition monitoring signal.

This work was supported in part by the U.S. National Science Foundation under Grants ECCS-1308045 and CMMI-1663562.

The authors are with the Power and Energy Systems Laboratory, Department of Electrical and Computer Engineering, University of Nebraska-Lincoln, Lincoln, NE 68588-0511 USA (e-mail: yayu.peng@huskers.unl.edu; wqiao3@unl.edu; lqu2@unl.edu).

the lost data samples in the transmitted signals can be random and their durations can be uncertain. Compared with single- or multiple-point random data loss, it is more challenging to recover the random data loss over a long period shown in Fig. 1. This problem will make the subsequent signal processing and condition monitoring difficult and may even lead to failure of condition monitoring. To improve the reliability of the remote wind turbine CMSs, it is urgent to solve the data loss problem.

The data loss problem has been addressed via three different approaches. The first approach is improving the reliability of the WSN communication hardware. For example, a multiple-antenna transmission is more reliable than a single-antenna transmission [8]. This, however, will increase hardware cost. The second approach is adopting an advanced communication protocol, such as the data loss notification protocol [9] to improve the communication reliability. However, this approach may increase system latency and power consumption. Moreover, the data loss problem can only be alleviated rather than completely avoided by these two approaches.

Instead of trying to avoid data loss during wireless communication, the third approach solves the data loss problem in WSNs by using a missing data recovery technique. The existing missing data recovery techniques can be grouped into statistical methods, artificial intelligence-based methods, and filter-based methods. For a statistical method, a mathematical model needs to be constructed from the historical data, and the performance of the missing data recovery is greatly influenced by the accuracy of the model constructed [10], [11]. Artificial intelligence techniques, such as artificial neural networks (ANNs) have been widely used to solve missing data recovery problems [12]. For example, an autoassociative neural network [13] and a radial basis function neural network [14] have been used for missing data recovery. The problem of data loss in wind turbine condition monitoring also has been addressed by using ANNs. For example, an ANN-based statistical learning framework was proposed in [15] for intelligent imputation of missing SCADA data for offshore wind farms. An ANN was also used in [16] for missing data imputation in structural health monitoring of offshore wind turbines. However, there are two limitations of the ANN-based methods. First, training ANNs requires sufficient historical data, which is not available in some real-world applications. Second, missing data recovery relies on the use of different types of data that have strong correlations and, thus, do not work for wind turbine CMSs with the sensor data that usually have weak correlations. In [17], a Kalman filter was designed to impute missing solar irradiance data. A fuzzy filter was also proven to be effective to estimate system states with missing measurements [18]. However, since the filter-based methods predict lost data recursively, they may not work for long-period data loss due to the accumulation of the prediction error over the lost data samples.

This paper proposes a novel compressive sensing (CS)-based missing-data-tolerant fault detection method to address the data loss problem in remote condition monitoring of wind turbines. The CS is an emerging sensing technique that can reconstruct sparse signals from measurements that are far fewer than those required in the traditional Nyquist sampling method [19]. The CS technique has been adopted in various applications, such as camera, medical imaging, and compressive sensor networks [20]-[22]. The proposed method consists of four modules: a signal conditioning module, a CS-based signal sampling module, a signal reconstruction module, and a fault detection module. The signal conditioning module converts the measured signals into the signals that are sparse in the frequency domain. The conditioned signals that are sparse in the frequency domain are then compressively sensed by the CS-based signal sampling module to generate the measurements of the conditioned signals. The measurements are transmitted wirelessly to the data receiving end, during which some data may be lost. Then, the signal reconstruction module reconstructs the original conditioned signals from their measurements received at the receiving end. The process is tolerant to data loss because the original conditioned signals can be reconstructed from their own measurements even when the measurements have high data loss rates during the wireless transmission. Moreover, the process does not need any historical data of the signals that is needed in existing missing data recovery methods. Finally, the reconstructed signals are used for wind turbine fault detection. To the best of the authors' knowledge, this is the first work of using the CS technique to solve the data loss problem in remote condition monitoring of wind turbines and the first method that is capable of missing-data-tolerant fault detection for wind turbines without the need for extra correlated signal(s) because each condition monitoring signal can be reconstructed from its own data even when the data has a high loss rate.

The remainder of this paper is organized as follows. Section II presents the proposed CS-based missing-data-tolerant fault detection method for remote condition monitoring of wind turbines. Section III presents the pseudocode of the proposed method. Section IV validates the proposed method for remote condition monitoring of two direct-drive wind turbines. Concluding remarks are presented in Section V.

II. Proposed CS-Based Missing-Data-Tolerant Fault Detection Method

The framework of the proposed CS-based missing-data-tolerant fault detection method for remote condition monitoring of wind turbines is shown in Fig. 2. It consists of four functional modules: signal conditioning, CS-based signal sampling, signal reconstruction, and fault detection. The condition monitoring signals, such as vibration, generator current and voltage, etc., are collected by the wireless sensor node installed in the wind turbine. Due to the time-varying shaft rotating speed caused by the variable wind condition, some of the measured signals, such as vibration and current signals are nonstationary, i.e., having time-varying frequencies. Moreover, the measured signals usually contain noise due to the harsh operating environment of the wind turbine. Both issues lead to low sparsity of the original signals in the time and frequency domains, where the sparsity of a signal can be measured by the ratio of the number of zero-valued data samples to the total number of data samples of the signal. In practice, due to the existence of noise (e.g., measurement noise and quantization noise), zero-valued data samples may not be exactly zero. To address this issue, a small

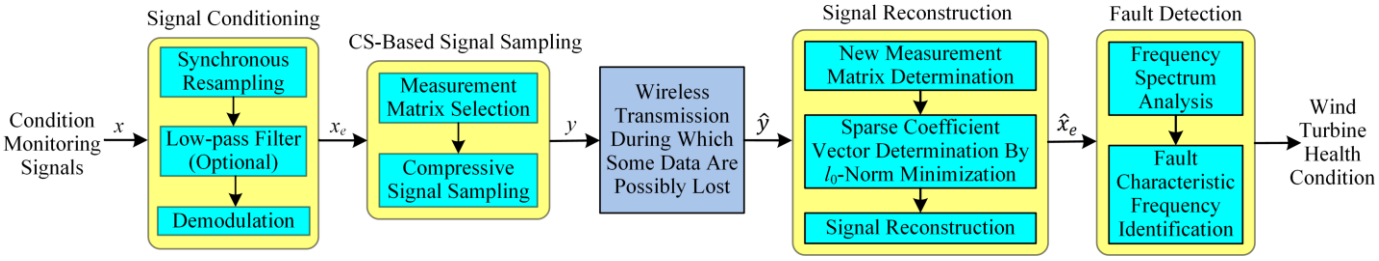

Fig. 2. Framework of the proposed CS-based missing-data-tolerant fault detection method for remote condition monitoring of wind turbines.

threshold can be established and the data samples whose values are lower than the threshold will be treated as zero-valued data samples for measuring the sparsity of the signal [23].

Since the CS method is only applicable to highly sparse signals, appropriate signal conditioning algorithms are firstly designed to increase the sparsity of the original signals. For generator current signals used in this paper and vibration signals, the signal conditioning module includes a synchronous resampling algorithm to convert the time-varying frequencies contained in the original signal x to be constant frequencies, an optional low-pass filter to alleviate the influence of the environment noise and the possible harmonics caused by the power electronic converter, and a demodulation algorithm to extract the envelope x_e of the resampled signal. The extracted envelope signal x_e contains possible fault characteristic frequency components, which modulate the fundamental frequency component in the original signal. Then, the CS-based signal sampling is performed on x_e by linearly projecting x_e on a selected measurement matrix. The resulting signal is denoted by y, which preserves the information in x_e and is called the measurements of x_e. The signal y is transmitted to the receiving end (gateway) through wireless communication. The signal received at the receiving end is denoted by $\hat{y}$ in which some data samples are possibly lost during the transmission. Then, the signal reconstruction is performed to recover the envelope signal x_e from the received signal $\hat{y}$ according to the CS technique. The reconstructed signal is denoted by $\hat{x}_e$. Finally, spectrum analysis is performed on the reconstructed signal $\hat{x}_e$. If one or more wind turbine fault characteristic frequencies are identified in the spectrum of $\hat{x}_e$, it indicates that the corresponding fault(s) occur in the wind turbine.

Compared with the traditional WSN-based CMSs [24], [25], the proposed method first conditions the collected signals and then transmits the measurements of the conditioned signals obtained from the CS rather than the collected original signals. Since the conditioned signals are sparse in frequency domain, it is possible to reconstruct the conditioned signals from their measurements according to the CS technique even though some of the measurements are lost during the wireless signal transmission. This makes the WSN-based CMS robust to data loss. The theoretical details of the proposed method are described as follows.

A. Signal Conditioning

Compressive sensing requires the signal to be sparse. Mathematically, a signal $x(t)$ is s-sparse when it has at most s nonzeros, i.e., $\|x(t)\|_0 \le s$, where $\|\cdot\|_0$ denotes the number of nonzero samples of the signal. The sparsity can be quantified by s. The smaller the value of s, the sparser the signal. In the wind turbine health condition monitoring, it is common to convert the signals, such as vibration and electrical signals, from time to frequency domain in order to identify the fault characteristic frequencies. However, many frequencies, including fault characteristic frequencies of the measured signals are proportional to the shaft rotational frequency (SRF) of the wind turbine [26]. Due to the time-varying SRF, the frequencies of the signals are time-varying, which causes a spectrum smearing problem because different time-varying frequencies will overlap with each other in the frequency spectrum of the signal $x(t)$, which is denoted as $X(f)$. As a consequence, the spectrum signal $X(f)$ has many nonzeros, meaning that the measured signal $x(t)$ has a low sparsity in the frequency domain.

To increase the sparsity of the measured signals in frequency domain, a synchronous resampling algorithm is firstly designed to convert the frequencies of the signals that vary with the SRF to be constant values. The algorithm consists of two steps: SRF estimation and angular resampling. The SRF can be estimated from the time-frequency distribution (TFD), defined as follows [27], of a measured stator current signal of a permanent-magnet synchronous generator (PMSG) or a rotor current signal of a doubly-fed inductor generator (DFIG), denoted as $c(t)$.

$$\mathrm{TFD}[c(t)] = |\mathrm{STFT}[c(t)](t,f)| \tag{1}$$

where STFT stands for short-time Fourier transform defined by

$$\mathrm{STFT}[c(t)](t,f) = \int_{-\infty}^{+\infty} c(\tau)h(\tau - t)e^{-j2\pi f\tau}d\tau \tag{2}$$

where $h(t)$ is a window function. The instantaneous fundamental frequency of the current signal, $f_c(t)$, is estimated by searching for the global maxima over the whole frequency range of the TFD along the time axis, as expressed by

$$f_c(t) = \arg\max_f \{\mathrm{TFD}[c(t)](t,f)\}. \tag{3}$$

Then, the SRF $f_r(t)$ of a PMSG is obtained by

$$f_r(t) = f_c(t)/p \tag{4}$$

The SRF $f_r(t)$ of a DFIG is obtained by

$$f_r(t) = [f_{s1} \pm f_c(t)]/p \tag{5}$$

where p is the number of pole pairs of the generator; f_{s1} is the fundamental frequency of the DFIG stator circuit; and + or – is used in (5) when the DFIG operates above or below the synchronous speed, respectively.

The angular resampling aims to resample an original equal-time-interval signal $x(t)$ at the time points relative to the equal-phase-increment shaft rotation. Define the initial shaft phase position of $x(t)$ to be $\theta(t_0) = 0$. Then, the relationship of

shaft phase position $\theta(t)$ versus time of $x(t)$ ($t \in T$) is established according the estimated SRF as follows.

$$\theta(t_i) = 2\pi \sum_{t=t_0}^{t=t_i} f_r(t)\Delta t, \;\; i = 1, 2, \cdots, P-1 \qquad (6)$$

where $T = [t_0, t_1, t_2, \ldots, t_{P-1}]$ is the vector of the sampling time points of $x(t)$ with a constant sampling time interval Δt; and P is the number of data samples of $x(t)$.

The shaft phase-time relationship of the resampled signal of $x(t)$ ($t \in T$) with a constant phase increment $\Delta\theta$, denoted as $x_r(t)$ ($t \in T'$), can be expressed as

$$\theta(\tau_i) = i \cdot \Delta\theta, \tau_i \in T' \qquad (7)$$

where $T' = [\tau_0, \tau_1, \tau_2, \ldots, \tau_{N-1}]$ is the vector of the resampling time points with varying intervals in general; N is the number of data samples of the resampled signal; and $\Delta\theta$ is determined by

$$\Delta\theta = \frac{\theta(t_{P-1})}{N} \qquad (8)$$

The value of N is selected according to the desired sampling frequency of the resampled signal, e.g., twice the highest fault characteristic frequency of interest, and can be different from P. If $N < P$, then the original signal $x(t)$ will be resampled with a lower sampling frequency, leading to a downsampling operation. This can reduce the computing burden and memory usage of the proposed fault detection method.

Then, the resampling time points contained in the vector T' are obtained by the cubic spline interpolation method according to the phase-time relationships expressed by (6) and (7). Using a cubic piecewise polynomial $\Theta(t)$ to represent the phase-time relationship (6), the element τ_i of T' can be obtained by solving the following equation.

$$\Theta(\tau_i) = \theta(\tau_i), \tau_i \in T' \qquad (9)$$

The data samples of the resampled signal $x_r(t)$ ($\forall\, t \in T'$) in the angle domain, $x_r[\theta(\tau_i)]$ ($\forall\, \tau_i \in T'$) are also obtained by the cubic spline interpolation method. Using another cubic piecewise polynomial $E(t)$ to represent the original signal $x(t)$ ($t \in T$), the new data sample $x_r[\theta(\tau_i)]$ can be obtained by solving the following equation.

$$x_r[\theta(\tau_i)] = E(\tau_i) \qquad (10)$$

The resampled signal is an order-tracked signal $x_r[\theta(t)]$ sampled in the angle domain with an equal phase increment $\Delta\theta$ and a time-domain signal $x_r(t)$ sampled with varying intervals for $\forall\, t \in T'$. Here the "order" $O(t)$ is defined to be a frequency of the signal normalized by the SRF $f_r(t)$ as follows.

$$O(t) = \frac{f(t)}{f_r(t)} \qquad (11)$$

where $f(t)$ is each time-varying frequency contained in the original signal $x(t)$. Since the characteristic frequencies used for fault detection are proportional to $f_r(t)$, the corresponding orders are constant. After the resampling, the time-varying SRF $f_r(t)$ becomes a constant frequency f_r', which is called the time-invariant SRF. Thus, according to (11), each time-varying frequency $f(t)$ contained in the original signal $x(t)$ is converted to a constant frequency in the resampled signal $x_r(t)$. Therefore, the spectrum smearing problem of the original signal $x(t)$ is solved by the resampled signal $x_r(t)$.

The resampled signal $x_r(t)$ contains the components at the constant fundamental frequency $f_c' = pf_r'$, some constant odd harmonics of f_c', fault-induced constant-frequency sidebands around f_c' and its harmonics, and some noise. Thus, compared to the frequency spectrum $X(f)$ of the original signal $x(t)$, the frequency spectrum $X_r(f)$ of the resampled signal $x_r(t)$ has much less nonzeros, meaning that the resampled signal has a much higher level of sparsity than the original signal in the frequency domain.

To further improve the sparsity level of the resampled signal $x_r(t)$, it is filtered using a low-pass filter and the resulting signal is denoted as $x_f(t)$. The bandwidth of the low-pass filter should be selected higher than the highest frequency of interest, such as the highest fault characteristic frequency.

Then, demodulation is performed on $x_f(t)$ to extract its envelope $x_e(t)$ using Hilbert transform, denoted as $H[\cdot]$ [27].

$$x_e(t) = \sqrt{\{x_f^2(t) + \{H[x_f(t)]\}\}^2} \qquad (12)$$

The envelope signal $x_e(t)$ only contains modulation frequency components of $x_r(t)$ in the low frequency range, including the possible fault characteristic frequency components of the wind turbine, but does not contain the fault-irrelevant fundamental component of $x_f(t)$. Thus, $x_e(t)$ has a higher sparsity level than $x_f(t)$ in frequency domain.

B. CS-Based Signal Sampling

The CS theory is based on the fact that a relatively small number of random projections of a sparse signal can contain most of its salient information [28]. The CS-based signal sampling of the N-point envelope signal x_e obtained in Section II.A is implemented via the following linear projection.

$$y = \phi x_e \qquad (13)$$

where $\phi \in R^{M \times N} (M \leq N)$ is called measurement matrix and $y \in R^M$ is the vector of linear measurements of x_e. If $M < N$, e.g., when some data in y is lost, the problem of reconstructing x_e from the measurements y using (13) is underdetermined and, therefore, cannot be solved to obtain the exact solution of x_e. An approximate solution of x_e can be obtained by the least squares method. However, if M is much smaller than N, e.g., there is significant data loss in y, the approximation error could be very large. To solve this underdetermined problem, compressive sensing adds a constraint of sparsity on the signal x_e. The constraint requires that the signal x_e must be sparse or can be transformed into another sparse signal so that it can be reconstructed from its measurements y by solving an optimization problem even if $M \ll N$ due to data loss or signal compression.

Besides the sparsity constraint on x_e, it is important to design the measurement matrix ϕ to ensure that y preserves the salient information of the signal x_e so that x_e can be reconstructed from y. This requires that ϕ satisfies the restricted isometry property (RIP) according to the CS theory. A matrix ϕ satisfies the RIP of order s if there exists a $\delta_s \in (0,1)$ such that

$$(1 - \delta_s)\|x_e\|_2^2 \leq \|\phi x_e\|_2^2 \leq (1 + \delta_s)\|x_e\|_2^2 \qquad (14)$$

holds for the s-sparse vectors x_e. When the RIP holds, the

matrix ϕ approximately preserves the Euclidean length of the signal x_e, i.e., the length of ϕx_e is bounded by $(1\pm\delta_s)x_e$. This implies that the pairwise distance between x_e and any other same-length sparse signal x_e' that is different from x_e is preserved in the measurement space. In other words, the approximation $\|y - y'\|_2^2 = \|\phi(x_e - x_e')\|_2^2 \approx \|x_e - x_e'\|_2^2$ holds, where y' is the measurement vector of x_e' obtained from (13). The RIP property of ϕ ensures that if the sparse signal x_e is identifiable from any other same-length sparse signal x_e', the measurements y of x_e is also identifiable from the measurements y' of x_e' because the distance between x_e and x_e' is preserved in the measurement space. Then, according to [28], x_e can be uniquely reconstructed from y. On the contrary, if the RIP property of ϕ does not hold, the distance between y and y' may be much smaller than the distance between x_e and x_e' or even close to zero. In this case, y is no longer identifiable from y' and, therefore, cannot be used to reconstruct x_e because the reconstructed signal may be x_e'.

If ϕ satisfies the RIP, a variety of algorithms can be applied to recover a sparse signal x_e from its measurements y [29]. It has been shown that a random matrix would satisfy the RIP with a high probability if its entries are chosen according to a Gaussian, Bernoulli, or more generally any sub-Gaussian distribution [29]. There are two benefits of using a random matrix to construct ϕ. First, the measurements are democratic, making it possible to recover x_e using any sufficiently large subset of the measurements. Thus, the loss or corruption of a fraction of the measurements would not influence the signal recovery. Second, if x_e is not sparse in time domain but is sparse in another domain spanned by some basis ψ, then x_e can be transformed into another domain by

$$x_e = \psi\alpha \tag{15}$$

where $\psi \in R^{N\times N}$ is the basis matrix and $\alpha \in R^{N\times 1}$ is the sparse coefficient vector with s nonzero values, which usually satisfies $s \ll N$. It is proved that if ϕ is a random matrix, $\phi\psi$ satisfies the RIP with a high probability [30].

Since the envelope signal x_e is not sparse in time domain but is sparse in frequency domain, ψ is selected to be the Fourier matrix defined in (16) so that (15) transforms x_e from time domain into frequency domain.

$$\psi = \begin{bmatrix} 1 & 1 & 1 & & 1 \\ 1 & \omega & \omega^2 & \cdots & \omega^{n-1} \\ \vdots & \vdots & \vdots & \ddots & \vdots \\ 1 & \omega^{n-1} & \omega^{2(n-1)} & \cdots & \omega^{(n-1)^2} \end{bmatrix} \tag{16}$$

where $\omega = e^{\frac{2\pi j}{N}}$. As a result, the vector of measurements y of the envelope signal x_e is obtained by

$$y = \phi x_e = \phi\psi\alpha = A\alpha \tag{17}$$

where $A \in R^{M\times N}$ is called sensing matrix, which satisfies the RIP as stated in the last paragraph. The measurements y are then sent wirelessly to the receiving node.

C. Signal Reconstruction

The M-length measurement vector y is subject to data loss during wireless transmission. The data loss could be random point data loss or random data loss over an uncertain period as illustrated in Fig. 3 in which the lost data in the received measurement vector $\hat{y}$ is masked by a white rectangle of the length N_l. The received signal $\hat{y}$ is an $\widehat{M}$-length vector that can be expressed as a linear projection of x_e below, where $\widehat{M} = M - N_l$ and N_l is the number of the lost data points in $\hat{y}$.

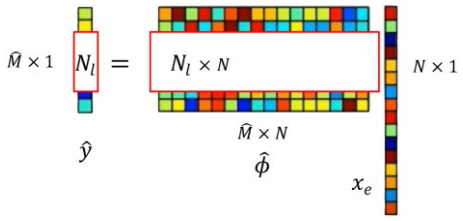

Fig. 3. Illustration of the CS-based signal sampling for the received measurement vector with data lost during wireless transmission.

$$\hat{y} = \hat{\phi}x_e = \hat{\phi}\psi\alpha = \hat{A}\alpha \tag{18}$$

where $\hat{\phi} \in R^{\widehat{M}\times N}$ is a new measurement matrix, which is a copy of ϕ but with the N_l rows corresponding to the positions of the lost data in y removed, as shown in Fig. 3. Since ϕ is a random matrix, the $\widehat{M}\times N$ matrix $\hat{\phi}$ is still a random matrix. So is the matrix $\hat{A} \in R^{\widehat{M}\times N}$, which satisfies the RIP. According to the CS theory, the received signal $\hat{y}$ can also be regarded as the measurements of x_e. It is pointed out in [31] that if any $2s$ columns of the $\widehat{M}\times N$ measurement matrix $\hat{\phi}$ are linearly independent, then the s-sparse signal α can be reconstructed uniquely from its measurements $\hat{y}$. The data loss can happen randomly at any positions of the received data and the signal reconstruction is insensitive to this randomness.

To recovered x_e from $\hat{y}$, the sparse coefficient vector α is firstly recovered as $\hat{\alpha}$ by solving the following l_0-norm minimization problem.

$$\hat{\alpha} = \arg\min\|\alpha\|_0 \quad \text{s.t. } \hat{y} = \hat{A}\alpha \tag{19}$$

where $\|\alpha\|_0$ denotes the number of nonzero elements in α.

However, the problem (19) is a non-deterministic polynomial-time hard (NP-hard) problem, which is difficult to solve. An approximate solution of (19) can be obtained by using the orthogonal matching pursuit (OMP) algorithm, which is presented in Table I, where $\emptyset$ is an empty set and supp(z) denotes the support of the vector z. The OMP algorithm begins by finding the column of $\hat{A}$ that is most correlated with the measurements $\hat{y}$ via the "initialize," "match," and "identify" steps with $l = 0$ in Table I. Then, the "match" and "identify" steps are repeated to correlate the columns in $\hat{A}$ with the residual of the signal $\hat{y}$, denoted as r^{l+1}, which is obtained in the "update" step by subtracting a partial estimate of the signal $\hat{y}$, denoted as $\hat{A}\alpha^{l+1}$, from the original signal $\hat{y}$. The stopping criterion is that either the predefined maximum number of iterations is reached or $\hat{y} \approx \hat{A}\hat{\alpha}$ is satisfied [32].

Once $\hat{\alpha}$ is obtained, the envelope signal x_e can be reconstructed as $\hat{x}_e$ by

$$\hat{x}_e = \psi\hat{\alpha} \tag{20}$$

The reconstruction error ξ between the reconstructed signal $\hat{x}_e$ and the original envelop signal x_e is defined as

$$\xi = \frac{\|\hat{x}_e - x_e\|_2}{\|x_e\|_2} \tag{21}$$

TABLE I
ALGORITHM OF ORTHOGONAL MATCHING PURSUIT [32]

Inputs: matrix $\hat{A}$, measurement vector $\hat{y}$, stopping criterion
Initialize: $r^0 = \hat{y}$, $\alpha^0 = 0$, $\Lambda^0 = \emptyset$, $l = 0$
While not converged **do**
Match: $h^l = \hat{A}^T r^l$
Identify: $\Lambda^{l+1} = \Lambda^l \cup \{\arg\max_k |h^l(k)|\}$
Update: $\alpha^{l+1} = \arg\min_{z:\mathrm{supp}(z)\subseteq\Lambda^{l+1}} \|\hat{y} - \hat{A}z\|_2$
$r^{l+1} = \hat{y} - \hat{A}\alpha^{l+1}$
$l = l + 1$
End while
Output: $\hat{\alpha} = \alpha^l$

D. Fault Detection

This paper does not aim at proposing a new fault detection algorithm for wind turbines. The fault detection module of the proposed method can be implemented by using the existing methods reported in the literature or used in industry, such as frequency or order spectrum analysis [3], [25], [26], anomaly detection [5], or machine learning-based classification [24], [27]. In this paper, the traditional frequency spectrum analysis method [3], [26] is adopted for the fault detection based on the identification of the fault characteristic frequencies in the amplitude spectrum of the reconstructed signal $\hat{x}_e$. In practice, fault characteristic frequencies of wind turbine drivetrain components, such as the shaft bearing fault characteristic frequencies given in Section IV.A, can be determined according to the geometries and rotating frequencies of the components [26], [27]. If a fault occurs, the corresponding characteristic frequency will appear as an impulse in the amplitude spectrum of $\hat{x}_e$. The impulses can be extracted by using an impulse detection method [26]. If an impulse is detected at a fault characteristic frequency, it indicates that the corresponding fault may occur. The final fault detection result can be obtained by comparing the amplitude of the impulse against a threshold, which can be determined from the historical failure cases. If the amplitude is lower than the threshold, it indicates that the fault has occurred but is not mature yet. Otherwise, if the amplitude exceeds the threshold, it indicates that the fault has become mature so that an alarm should be triggered and maintenance is needed.

Since no parameter tuning is needed in the CS-based signal sampling and reconstruction processes, the proposed method has a merit of parameter tuning free. Thus, the proposed method has no parameter that will affect fault detection efficacy, which is mainly affected by the data loss rate itself.

III. PSEUDOCODE OF THE PROPOSED METHOD

The pseudocode of the proposed method is shown in Table II. The signal conditioning and CS-based signal sampling are conducted at the sending end, and the signal reconstruction and fault detection are conducted at the receiving end of the remote condition monitoring system. The purpose of signal conditioning is to increase the sparsity of the signal. The compressive measurements of the conditioned signal are transmitted. The received measurements may be incomplete due to data loss. Signal reconstruction is conducted using the received measurements. Fault detection is carried out using the frequency spectrum of the reconstructed data. The output includes a Boolean indicating whether a fault is detected and if a fault is detected, fault type will also be identified.

TABLE II
PSEUDOCODE OF THE PROPOSED METHOD

Initialize: fault alarm = false
While fault alarm == false **do**
%%%% Operations at Sending End %%%%
Input: condition monitoring signal x.
Signal Conditioning (SC) to increase signal sparsity:
SRF estimation (SRFE): $f_r \leftarrow \mathrm{SRFE}(x)$.
Angular resampling (AR): $x_r \leftarrow \mathrm{AR}(x, f_r)$.
Low-pass filtering (LPF): $x_f \leftarrow \mathrm{LPF}(x_r)$.
Demodulation: $x_e \leftarrow \sqrt{\{x_f^2 + \{H[x_f]\}\}^2}$.
CS-based Signal Sampling:
Measurement matrix generation: use Gaussian distribution to generate entries of the $M \times N$ matrix ϕ.
Compressive measurements generation: $y = \phi x_e$.
Send: compressive measurements y
%%%% Data Transmission %%%%
%%%% Operations at Receiving End %%%%
Receive: compressive measurements $\hat{y}$
Signal Reconstruction by OMP:
Measurement matrix generation: generate $\hat{\phi}$ from ϕ according to locations of lost data in $\hat{y}$.
Generation of $\hat{M} \times N$ matrix $\hat{A}$: $\hat{A} = \hat{\phi}\psi$.
Signal reconstruction: $\hat{\alpha} \leftarrow \mathrm{OMP}(\hat{y}, \hat{A})$.
Fault Detection:
If: $\hat{\alpha}$ contains fault characteristic frequencies
Then: fault alarm = true and fault type identification according to the characteristic frequency.
Output: fault alarm and detected fault type.

IV. APPLICATION OF THE PROPOSED METHOD TO REMOTE CONDITION MONITORING OF DIRECT-DRIVE WIND TURBINES

A. Experiment Setup

The proposed method is applied to commercial direct-drive wind turbines in the field, where each wind turbine is equipped with a PMSG and a WSN-based remote CMS, as shown in Fig. 4. The WSN consists of a wireless sensor node (Model: V-Link® -LXRS®) installed on the nacelle of the wind turbine and a gateway (Model: WSDA®-1500-LXRS®). The sensor node collects the data of one-phase PMSG stator current signal once per hour with a sampling frequency of 1000 Hz. The length of each data record is 15 seconds. Thus, each data record contains a total of 15000 data samples. The collected current signal is processed by the proposed signal conditioning algorithm to obtain its envelope signal, which is then processed by CS-based signal sampling algorithm to obtain the measurement signal. The data of the measurement signal is transmitted wirelessly from the sensor node to the gateway. The gateway receives the data and uploads the data to a web server SensorCloud™ on which the data is stored. A lab computer is connected to the SensorCloud™ server through the Internet to

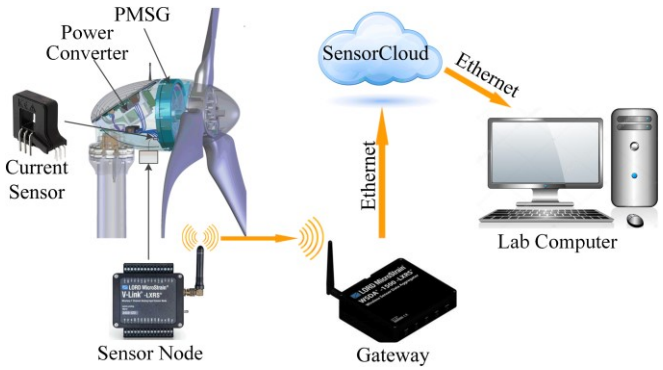

Fig. 4. A commercial direct-drive wind turbine equipped with the proposed WSN-based remote CMS in the field.

access the data of the measurement signal, which is then used by the CS-based signal reconstruction program running on the computer to recover the envelope of the current signal. Finally, the recovered current envelope signal is used for remote fault detection of the wind turbine.

The data collected from a Skystream 3.7 wind turbine and an Air Breeze wind turbine were used to validate the proposed method. The Skystream 3.7 wind turbine has a cage fault in a shaft bearing and the corresponding characteristic frequencies can be computed as follows [33].

$$f_{\mathrm{FTFO}} = \frac{f_r'}{2}\left(1 - \frac{d}{D}\cos\gamma\right) \tag{22}$$

$$f_{\mathrm{FTFI}} = \frac{f_r'}{2}\left(1 + \frac{d}{D}\cos\gamma\right) \tag{23}$$

where f_{FTFO} and f_{FTFI} are characteristic frequencies of bearing cage fault when the damaged cage touches the outer and inner rings, respectively, d is the diameter of the rolling elements, D is the bearing pitch diameter, and γ is the contact angle. The Air Breeze wind turbine has a shaft bearing outer race fault whose characteristic frequency f_{BPFO} can be computed as:

$$f_{\mathrm{BPFO}} = \frac{f_r'}{2} N_b \left(1 - \frac{d}{D}\cos\gamma\right) \tag{24}$$

where N_b is the number of bearing rolling elements.

B. Experimental Results of a Bearing Cage Fault

For the Skystream 3.7 wind turbine, the geometry parameters of the shaft bearing are D = 65 mm, d = 12.7 mm, and γ = 0. The time-invariant SRF is $f_r' = 2$ Hz in this experiment. According to (22) and (23), the bearing cage fault characteristic frequencies are calculated as f_{FTFO} = 0.8 Hz and f_{FTFI} = 1.2 Hz.

Fig. 5 shows the amplitude spectrum around the fundamental frequency of the generator stator current signal measured on February 4, 2016. Due to the time-varying shaft rotating speed of the wind turbine, the fundamental frequency distributes over a range from 42 Hz to 46 Hz and cannot be distinguished from its sidebands that contain the bearing fault characteristic frequencies, which causes a spectrum smearing problem and many impulses in the amplitude spectrum in Fig. 5. Thus, the sparsity of the current signal in frequency domain is low. To measure the sparsity of this amplitude spectrum while taking noise into consideration, a threshold with the amplitude to be 10% of the peak value of the spectrum is chosen, as shown in Fig. 5. The amplitude spectrum exceeds the threshold when the frequency is between 42-46 Hz. The sparsity of the amplitude

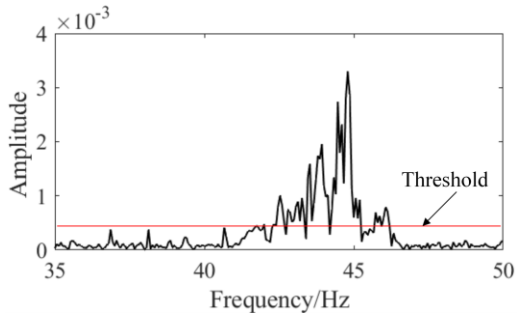

Fig. 5. Amplitude spectrum of the generator stator current signal measured on February 4, 2016 around its fundamental frequency.

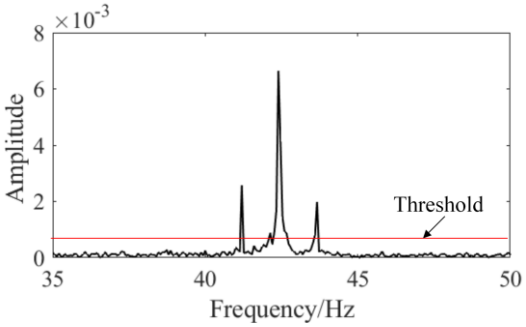

Fig. 6. Amplitude spectrum of the resampled current signal around its fundamental frequency.

spectrum is measured to be 0.7.

The synchronous resampling algorithm is used to solve the spectrum smearing problem. The amplitude spectrum of the resampled current signal with the sampling frequency the same as that of the original current signal is shown in Fig. 6 in which the frequency components are converted to single impulses by the synchronous resampling. Two sidebands around the fundamental frequency f_c' = 42.4 Hz are clearly identified at 41.2 Hz and 43.6 Hz in Fig. 6, meaning that the fundamental frequency f_c' is modulated by a frequency of 1.2 Hz, which is close to one of the bearing cage fault characteristic frequencies $f_{\mathrm{FTFI}} = 1.206$ Hz, indicating that the cage of the shaft bearing damaged. By using a threshold established in the same way in Fig. 5, the sparsity of the amplitude spectrum in Fig. 6 is increased to 0.94 because there are fewer values exceeding the threshold. Thus, the resampled current signal has a higher sparsity than the original current signal in frequency domain.

Since the bearing characteristic frequencies are much lower than the 1000 Hz sampling frequency of the original current signal, the number of data samples of the resampled current signal is reduced to 1500, which is only 10% of the 15000 data samples of the original current signal, namely, the resampled current signal is downsampled to 100 Hz. This reduces the computational time for the CS-based signal sampling and reconstruction, and save the memory space of the WSN. To further increase the sparsity level and reduce the noise of the current signal, a filter is applied to the resampled current signal to remove its high-frequency noise. Then, the envelope of the filtered resampled current signal is obtained via the Hilbert transform. The obtained current envelope signal mainly contains the fault-induced characteristic frequency and does not contain the fundamental frequency of the current signal. The

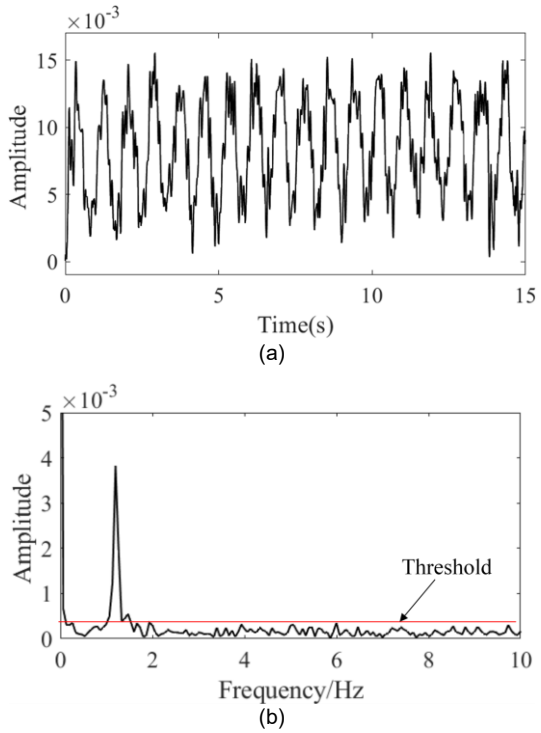

Fig. 7. Resampled current envelope signal: (a) time-domain samples and (b) amplitude spectrum.

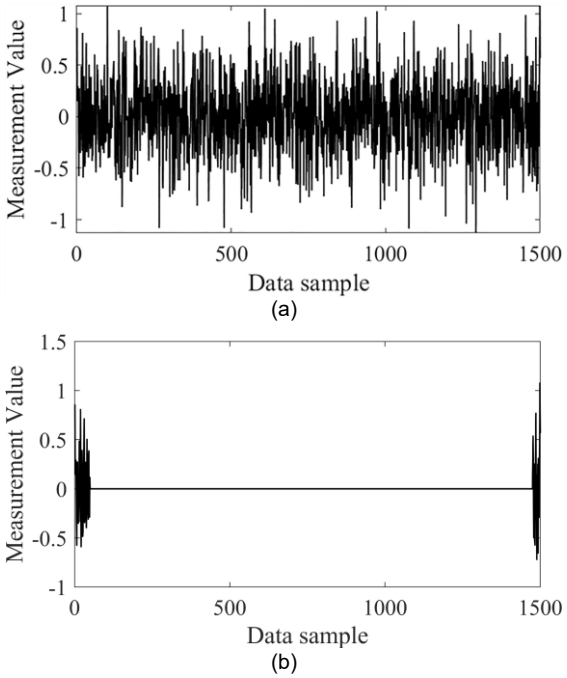

Fig. 8. Measurements of the resampled current envelope signal: (a) complete data samples and (b) incomplete data samples with a 95% data loss rate.

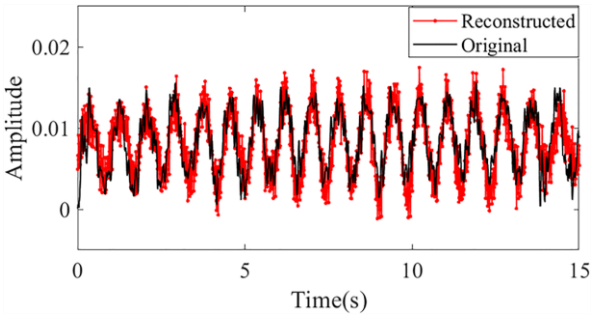

Fig. 9. Comparison of the reconstructed and original resampled current envelope signals.

waveform and amplitude spectrum of the resampled current envelope signal are shown in Fig. 7. The bearing cage fault characteristic frequency f_{FTFI} is the dominant in the amplitude spectrum. By using a threshold established in the same way in Figs. 5 and 6, the sparsity of the amplitude spectrum in Fig. 7 is increased further to 0.96 because only the 1.2Hz component exceeds the threshold. Thus, the resampled current envelope signal has a much higher sparsity than the original current signal shown in Fig. 5 and also a higher sparsity than the resampled current signal shown in Fig. 6 in frequency domain.

Then, the CS-based signal sampling is performed on the resampled current envelope signal and the resulting measurement signal is shown in Fig. 8(a). Assuming that 95% samples of the measurement signal are lost during the wireless transmission; and the beginning and end positions of the lost data are randomly selected, as displayed in Fig. 8(b), where the lost data points are filled by zero values. By applying the proposed data reconstruction method, the resampled current envelope signal is reconstructed from the incomplete measurements, as shown in Fig. 9 in comparison with the original resampled current envelope signal. The reconstruction error is 0.304 according to (21). Fig. 10 shows the amplitude spectrum of the reconstructed resampled current envelope signal, where the bearing cage fault characteristic frequency shown in Fig. 7(b) is also identified and the fault characteristic frequency components in Fig. 10 and 7(b) have the same amplitude. These results indicate that the bearing health information is recovered in the reconstructed resampled current envelope signal. Therefore, the proposed method is effective for remote condition monitoring of the wind turbine even when the condition monitoring signal has significant data loss.

Fig. 11 shows the curve of reconstruction error versus data loss rate of the received measurements of the resampled current envelope signal in this experiment. The reconstruction error is less than 0.3 even when the data loss rate is less than 95%, but increases dramatically when the data loss rate exceeds 95%. The result indicates that the proposed method has strong tolerance to missing data with the loss rate up to 95%.

Fig. 12 shows the case when the resampled current envelope signal shown in Fig. 7(a) instead of the measurements of the resampled current envelope signal shown in Fig. 8(a) is transmitted wirelessly and 95% data samples of the received resampled current envelope signal happen to be lost, as illustrated in Fig. 12(a). The spectrum of the received resampled current envelope signal is shown in Fig. 12(b), in which the fault characteristic frequency contained in the original envelope signal shown in Fig. 7(b) cannot be identified. The results in Figs. 7, 9, 10 and 12 demonstrate that in order to achieve missing-data tolerance in the remote condition monitoring of the wind turbine, it is necessary and effective to use the proposed CS-based fault detection method. Therefore, the proposed method can improve the reliability and robustness of the remote wind turbine CMS.

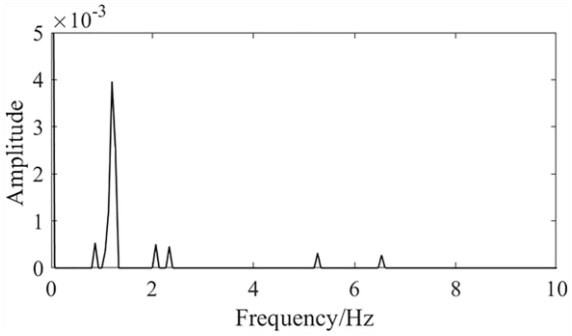

Fig. 10. Amplitude spectrum of the reconstructed current envelope signal.

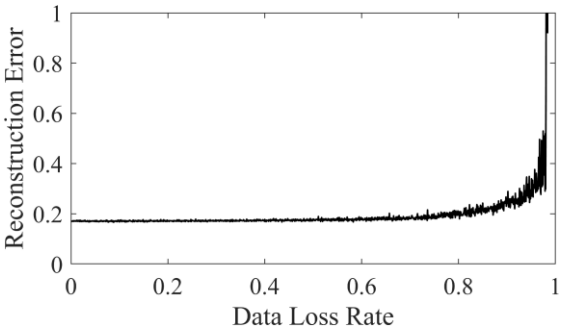

Fig. 11. Curve of reconstruction error versus data loss rate.

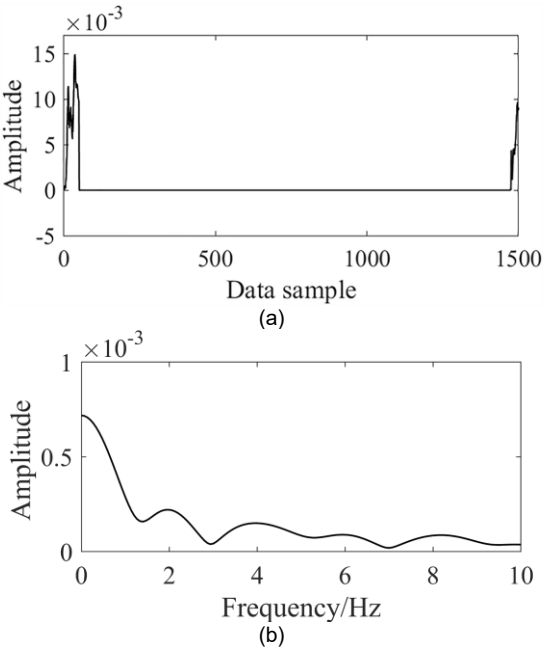

Fig. 12. Resampled current envelope signal with a 95% data loss rate: (a) time-domain samples and (b) amplitude spectrum.

C. Experimental Results of a Bearing Outer Race Fault

For the Air Breeze wind turbine, the geometry parameters of the shaft bearing are D = 33 mm, d = 8 mm, N_b= 8, and γ = 0. The time-invariant SRF is f_r' = 10 Hz in this test. According to (24), the bearing outer race fault characteristic frequency is $f_{\mathrm{BPFO}} \approx 30$ Hz. The amplitude spectrum of the resampled current envelope signal is shown in Fig. 13(a), where the 30Hz fault characteristic frequency is clearly identified. The sparsity

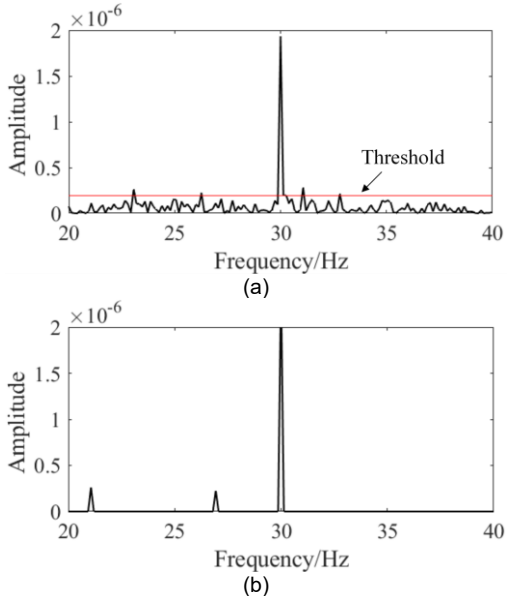

Fig. 13. Amplitude spectra of (a) resampled current envelope signal and (b) reconstructed current envelope signal when the measurement signal has 90% data loss rate during wireless transmission.

of the amplitude spectrum is measured to be 0.93. By using the proposed method, the bearing outer race fault can be detected as long as the data loss rate of the received measurement signal does not exceed 90%. Fig. 13(b) shows the amplitude spectrum of the reconstructed resampled current envelope signal when the measurement signal has a 90% data loss rate during wireless transmission, where the 30Hz fault characteristic frequency is also clearly identified. The result again validates the proposed method for missing-data-tolerant fault detection.

V. Conclusion

A compressive sensing-based missing-data-tolerant fault detection method for remote condition monitoring of wind turbines was proposed. The compressive sensing technique requires the signal to be sparse. To satisfy this requirement, signal conditioning was performed on the condition monitoring signals. The conditioned signals are sparser than the original signals in frequency domain. Then, measurements of the conditioned signals were obtained by using the compressive sensing-based sampling algorithm, transmitted wirelessly to a gateway of the wireless sensor network, and further transmitted to and saved on a data sever of the remote condition monitoring system. Due to the interference in wireless communication, the measurements might be partially lost during the data transmission. The conditioned signals were then reconstructed from their measurements received using the proposed method for the wind turbine fault detection.

The effectiveness of the proposed method was verified by using the data of a one-phase generator stator current signal collected from the remote condition monitoring systems of two direct-drive wind turbines in the field with a shaft bearing cage fault and a shaft bearing outer race fault, respectively. Field test results showed that the original current signal could not be used directly for the wind turbine fault detection via frequency spectrum analysis; the resampled current envelope signal

obtained from the signal conditioning module of the proposed method was effective for the wind turbine fault detection via frequency spectrum analysis; the resampled current envelope signal reconstructed from its measurements by the proposed method was also effective for the wind turbine fault detection, even when 95% or 90% of the measurements were lost during the wireless data transmission. Compared to the existing methods that use and transmit the collected original signals for remote condition monitoring, the proposed method is more reliable and more robust to high levels of data loss. Moreover, compared to the existing methods that require other signals and training to recover the lost data of a signal for wind turbine fault detection, the proposed method does not need any other signals or training for reconstructing the condition monitoring signal from its own measurements with lost data.

If the data loss rate is extremely high, such as over 95% or 90% in this work, the proposed method may not work properly. In this circumstance, the use of more advanced (i.e., more expensive) wireless sensor network hardware or other correlated signals would be needed to solve the data loss problem. In this paper, the fault detection was carried out by using the reconstructed signal. Future work can be carried out to develop fault detection algorithms using the received measurement signal directly without the signal reconstruction step, which can save computational resources. Moreover, this paper focused on solving the data loss problem instead of developing a new fault detection/diagnosis algorithm. In the future work, advanced fault diagnosis algorithms, such as those based on machine learning techniques, can be developed for identification of fault types, locations, severity, etc. using the received measurement signals or reconstructed signals.

REFERENCES

[1] R. Wiser and M. Bolinger, "2012 wind technologies market report," Lawrence Berkeley Nat. Lab., Tech. Report, Aug. 2015.

[2] W. Qiao and D. Lu, "A survey on wind turbine condition monitoring and fault diagnosis-Part I: Components and subsystems," *IEEE Trans. Ind. Electron.*, vol. 62, no. 10, pp. 6536-6545, Oct. 2015.

[3] E. Artigao, A. Honrubia-Escribano, and E. Gómez-Lázaro, "In-service wind turbine DFIG diagnosis using current signature analysis," *IEEE Trans. Ind. Electron.*, vol. 67, no. 3, pp. 2262-2271, Mar. 2020.

[4] J. Liu, F. Qu, X. Hong, and H. Zhang, "A small-sample wind turbine fault detection method with synthetic fault data using generative adversarial nets," *IEEE Trans. Ind. Informat*., vol. 15, no. 7, pp. 3877-3888, Jul. 2019.

[5] X. Jin, Z. Xu, and W. Qiao, "Condition monitoring of wind turbine generators using SCADA data analysis," *IEEE Trans. Sustain. Energy*, vol. 12, no. 1, pp. 202-210, Jan. 2021.

[6] V. C. Gungor, B. Lu, and G. P. Hancke, "Opportunities and challenges of wireless sensor networks in smart grid," *IEEE Trans. Ind. Electron.*, vol. 57, no. 10, pp. 3557-3564, Oct. 2010.

[7] Y. Bao, H. Li, X. Sun, Y. Yu, and J. Ou, "Compressive sampling based data loss recovery for wireless sensor networks used in civil structural health monitoring," *Struct. Health Monitor.*, vol. 12, no. 1, pp. 78-95, 2013.

[8] J. Mietzner, R. Schober, L. Lampe, W. H. Gerstacker, and P. A. Hoeher, "Multiple-antenna techniques for wireless communications-a comprehensive literature survey," *IEEE Comm. Surveys & Tutorials*, vol. 11, no. 2, pp. 87-105, Jun. 2009.

[9] S. Saravanan and E. Karthikeyan, "A protocol to improve the data communication over wireless network," *International Journal of Wireless & Mobile Networks*, vol. 3, no. 5, pp. 95-112, Oct. 2011.

[10] X. Huang and Q. Zhu, "A pseudo-nearest-neighbor approach for missing data recovery on Gaussian random data sets," *Pattern Recognition Letters*, vol. 23, no. 13, pp. 1613-1622, Nov. 2002.

[11] R. J. A. Little and D. B. Rubin, *Statistical Analysis with Missing Data*, New Jersey, USA: John Wiley & Sons, 2014.

[12] T. Marwala, *Computational Intelligence for Missing Data Imputation, Estimation, and Management: Knowledge Optimization Techniques*, New York, USA: IGI Global Publications, Information Science Reference Imprint, 2009.

[13] W. Qiao, R. G. Harley, and G. K. Venayagamoorthy, "Fault-tolerant indirect adaptive neurocontrol for static synchronous series compensator in a power network with missing sensor measurements," *IEEE Trans. Neural Networks*, vol. 19, no. 7, pp. 1179-1195, Jul. 2008.

[14] B. Hong and C. H. Chen, "Radial basis function neural network-based nonparametric estimation approach for missing data reconstruction of non-stationary series," in *Proc. International Conference on Neural Networks and Signal Processing*, Dec. 2003, pp. 75-78.

[15] X. Liu, Z. Zheng, Z. Zhang, and Z. Cao, "A statistical learning framework for the intelligent imputation of offshore wind farm missing SCADA data," in *Proc 8th Renewable Power Generation Conference*, Oct. 2019, pp. 1-4.

[16] M. Martinez-Luengo, M. Shafiee, and A. Kolios, "Data management for structural integrity assessment of offshore wind turbine support structures: Data cleansing and missing data imputation," *Ocean Engineering*, vol. 173, pp. 867-883, Feb. 2019.

[17] H. Demirhan and Z. Renwick, "Missing value imputation for short to mid-term horizontal solar irradiance data," *Applied Energy*, vol. 225, pp. 998-1012, Sep. 2018.

[18] G. Koo, J. Park, and Y. Joo, "Sampled-data H_∞ fuzzy filtering for nonlinear systems with missing measurements," *Fuzzy Sets and Systems*, vol. 316, pp. 82-98, Jun. 2017.

[19] D. Donoho, "Compressed sensing," *IEEE Trans. Inform. Theory*, vol. 52, no. 4, pp. 1289-1306, Apr. 2006.

[20] M. F. Duarte, M. A. Davenport, D. Takhar, J. N. Laska, T. Sun, K. F. Kelly, and R. G. Baraniuk, "Single-pixel imaging via compressive sampling," *IEEE Signal Processing Magazine*, vol. 25, no. 2, pp. 83-91, Mar. 2008.

[21] X. Zhu, Z. Zhao, J. Wang, J. Song, and Q. H. Liu, "Micro-induced thermal acoustic tomography for breast tumor based on compressive sensing," *IEEE Trans. Biomed. Eng.*, vol. 60, no. 5, pp. 1298-1307, May 2013.

[22] Y. Tang, B. Zhang, T. Jing, D. Wu, and X. Cheng, "Robust compressive data gathering in wireless sensor networks," *IEEE Trans. Wireless Commun.*, vol. 12, no. 6, pp. 2754-2761, Jun. 2013.

[23] N. Hurley and S. Rickard, "Comparing measures of sparsity," *IEEE Trans. Inf. Theory*, vol. 55, no. 10, pp. 4723-4741, Oct. 2009.

[24] L. Lu, Y. He, T. Wang, T. Shi, and Y. Ruan, "Wind turbine planetary gearbox fault diagnosis based on self-powered wireless sensor and deep learning approach," *IEEE Access*, vol. 7, pp. 119430-119442, Aug. 2019.

[25] J. Wang, Y. Peng, W. Qiao, and J. L. Hudgins, "Bearing fault diagnosis of direct-drive wind turbines using multiscale filtering spectrum," *IEEE Trans. Ind. Appl.*, vol. 53, no. 3, pp. 3029-3038, May-Jun. 2017.

[26] X. Gong and W. Qiao, "Current-based mechanical fault detection for direct-drive wind turbines via synchronous sampling and impulse detection," *IEEE Trans. Ind. Electron.*, vol. 62, no. 3, pp. 1693-1702, Mar. 2015.

[27] F. Cheng, J. Wang, L. Qu, and W. Qiao, "Rotor-current-based fault diagnosis for DFIG wind turbine drivetrain gearboxes using frequency analysis and a deep classifier," *IEEE Trans. Ind. Appl.*, vol. 54, no. 2, pp 1062-1071, Mar.-Apr. 2018.

[28] J. Romberg. A survey of compressive sensing and applications [Online]. Available: https://cpb-us-w2.wpmucdn.com/sites.gatech.edu/dist/2/436/files/2016/10/05-csoverview.pdf.

[29] M. Davenport, M. Duarte, Y. Eldar, and G. Kutyniok, "Introduction to compressed sensing," in *Compressed Sensing: Theory and Applications*. Cambridge, U.K. Cambridge University Press, 2011.

[30] E. J. Cadens and M. B. Wakin, "An introduction to compressive sampling," *IEEE Signal Processing Magazine*, vol. 25, no. 2, pp. 21-30, March 2008.

[31] T. Tao. Compressed sensing [Online]. Available: http://www.math.hkbu.edu.hk/~ttang/UsefulCollections/compressed-sensing1.pdf.

[32] M. A. Davenport and M. B. Wakin, "Analysis of orthogonal matching pursuit using the restricted isometry property," *IEEE Trans. Inf. Theory*, vol. 56, no. 9, pp. 4395-4401, Sep. 2010.

[33] S. J. Lacey, "An overview of bearing vibration analysis," *Maintenance Asset Manage.*, vol. 23, no. 6, pp. 32-42, Nov./Dec. 2008.

Yayu Peng (S'13) received the B.Eng. degree in electrical engineering from Chongqing University, Chongqing, China, in 2013. He is currently working toward the Ph.D. degree in the Department of Electrical and Computer Engineering, University of Nebraska–Lincoln, Lincoln, NE, USA.

He was a research and development intern at the Global Energy Interconnection Research Institute North America (GEIRINA) in 2018 and the New York Power Authority (NYPA) in 2020. His research interests include renewable energy systems, condition-based maintenance, and intelligent fault diagnosis and prognosis.

Wei Qiao (S'05–M'08–SM'12–F'20) received the B.Eng. and M.Eng. degrees in electrical engineering from Zhejiang University, Hangzhou, China, in 1997 and 2002, respectively, the M.S. degree in high-performance computation for engineered systems from Singapore-MIT Alliance, Singapore, in 2003, and the Ph.D. degree in electrical engineering from the Georgia Institute of Technology, Atlanta, GA, USA, in 2008.

Since August 2008, he has been with the University of Nebraska–Lincoln, Lincoln, NE, USA, where he is currently a Professor with the Department of Electrical and Computer Engineering. His research interests include renewable energy systems, smart grids, condition monitoring, power electronics, electric motor drives, energy storage systems, and emerging electrical energy conversion devices. He is the author or coauthor of more than 260 papers in refereed journals and conference proceedings and holds 11 U.S. patents issued. Dr. Qiao was a recipient of the 2010 U.S. National Science Foundation CAREER Award and the recipient of the 2010 IEEE Industry Applications Society Andrew W. Smith Outstanding Young Member Award.

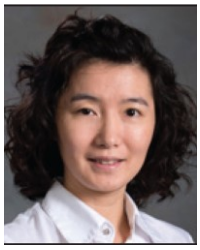

Liyan Qu (S'05–M'08–SM'17) received the B.Eng. (with the highest distinction) and M.Eng. degrees in electrical engineering from Zhejiang University, Hangzhou, China, in 1999 and 2002, respectively, and the Ph.D. degree in electrical engineering from the University of Illinois at Urbana–Champaign, Champaign, IL, USA, in 2007.

From 2007 to 2009, she was an Application Engineer with Ansoft Corporation, Irvine, CA, USA. Since January 2010, she has been with the University of Nebraska−Lincoln, Lincoln, NE, USA, where she is currently an Associate Professor with the Department of Electrical and Computer Engineering. Her research interests include energy efficiency, renewable energy, numerical analysis and computer aided design of electric machinery and power electronic devices, dynamics and control of electric machinery, and magnetic devices. Dr. Qu was a recipient of the 2016 U.S. National Science Foundation CAREER Award.